JOURNAL OF MATERIALS SCIENCE **33** (1998) 5433–5439

Calcium hydroxyapatites: evaluation of sorption properties for cadmium ions in aqueous solution

S. MANDJINY, K. A. MATIS, A. I. ZOUBOULIS
Division of Chemical Technology, Department of Chemistry, Aristotle University, 54006 Thessaloniki, Greece

M. FEDOROFF,* J. JEANJEAN, J. C. ROUCHAUD
Centre National de la Recherche Scientifique, Centre d'Etudes de Chimie Métallurgique, 15 rue Georges Urbain, 94407 Vitry-sur-Seine, France
E-mail: fedoroff@glvt-cnrs.fr

N. TOULHOAT, V. POTOCEK, C. LOOS-NESKOVIC
Commissariat à l'Energie Atomique, Centre National de la Recherche Scientifique, Laboratoire P. Sue, Centre d'Etudes de Saclay, 91191 Gif-sur-Yvette, France

P. MAIRELES-TORRES, D. JONES
Laboratoire des Agrégats Moléculaires et Matériaux Inorganiques, Université de Montpellier II, Place Eugène Bataillon, 34095 Montpellier, France

The efficiency and mechanisms of cadmium sorption on two synthetic calcium hydroxyapatites from aqueous solution were investigated. Both hydroxyapatites remove cadmium from aqueous solutions with an efficiency higher than 99.5% at pH 5–6. The mechanisms of cadmium sorption were studied using batch experiments, X-ray diffraction, scanning electron microscopy and nuclear microprobe. Cadmium is incorporated into the hydroxyapatite structure via diffusion and ion exchange. Once cadmium is sorbed, cadmium-containing hydroxyapatites can be separated from the liquid phase by flocculation. Thus hydroxyapatite can potentially be used for remediating contaminated water and industrial wastes. The fact that cadmium is incorporated into the bulk of the apatite is important in the context of the safe storage of used sorbent material.

1. Introduction

Cadmium is one of the major heavy toxic elements which may be found in surface and underground waters. The main sources of contamination are industrial wastes and phosphate fertilizers. Cadmium is a common impurity found in natural phosphates used for the manufacture of fertilizers [1]. One of the main toxic effects of cadmium is the interaction with the biological apatites of bones, leading to a disease producing effects similar to osteoporosis [2, 3]. When cadmium is present in natural waters, its migration is controlled by several equilibria between the liquid phase and solid matter, including phosphate phases [4]. It is, therefore, of major interest to study the interaction of cadmium ions in aqueous solution with apatites and other insoluble phosphates.

Hydroxyapatite can be used to remediate cadmium-contaminated waters and liquid wastes. It can also be used as a barrier to minimize cadmium migration from cadmium-containing solid wastes or from cadmium-contaminated soils. Previous investigations indicate that calcium hydroxyapatites are able to sorb cadmium and other toxic metal ions from aqueous solutions [3, 5–13]. The present studies were performed in order to evaluate the potential interest of apatites and to study the sorption mechanisms, for which several processes have been proposed: superficial sorption, ion exchange, precipitation.

In our previous studies [11, 13], we confirmed the ability of apatites to immobilize cadmium from aqueous solutions. Nearly 100% cadmium removal was found for dilute solutions [13]. Using structural analysis, the crystallographic sites of the apatite in which cadmium is sorbed, could be localized [11]. However, the process leading to the substitution of calcium sites by cadmium is still not clear and only a small part of the available sites can be substituted. More recently, using measurements performed by a nuclear microprobe [14], it was shown that cadmium is really incorporated into the bulk of the apatite particles. A pH-dependent modification of the apatite stoichiometry also takes place during sorption [15].

Two types of hydroxyapatites have been selected for the present study. One apatite, with well-defined and large particles, was used for the study of sorption

*Author to whom all correspondence should be addressed.

mechanisms. The other, available in larger quantities and at lower cost, but with small particles, was chosen for liquid decontamination testing. The properties of these two apatites are compared. In order to understand the sorption mechanisms, we used a multidisciplinary approach with several techniques such as batch sorption experiments, X-ray diffraction, scanning electron microscopy and nuclear microprobe.

During the treatment of contaminated waters after the sorption of cadmium on hydroxyapatite particles, the subsequent solid–liquid separation process could face technological problems, especially with a sorbent with small particle size (average diameter 2.5 μm). In order to circumvent these problems, we have tested a flocculation technique. This technique has to be optimized so that aggregates (flocs) of a certain size, strength and density should be formed. Although several methods are available for measuring the degree of flocculation and selecting the optimal dosage of flocculants [16], generally, the fundamental understanding of flocculant reagent action under dynamic conditions is limited. In a similar application, the flocculation behaviour of fine bentonite particles used for the removal of Cd^{2+}, Fe^{2+} and Cu^{2+} ions was examined by adding a cationic surfactant and a poly-acrylamide [17]. Flotation of cadmium as hydroxide, but in the absence of an inorganic sorbent has been previously studied [18]. The investigation of the possibility of flocculation of cadmium-loaded ultra-fine particles of hydroxyapatites is presented in the present paper with selected preliminary results.

2. Experimental procedure

2.1. Materials

Two commercial synthetic hydroxyapatites were used, one from "Bio-Rad," referenced DNA Grade Bio-Gel HTP 130-0420, another from Merck, referenced 2196. These solids are referred to here as BR and MK, respectively. The BR powder was sieved under water flow and particles of diameter ranging from 36–71 μm were selected. The MK apatite was not sieved. It was composed of small particles of diameters less than 25 μm with an average at 2.5 μm [13]. Specific surface area measurements performed by the nitrogen BET method lead to 52 $m^2\,g^{-1}$ for MK and 72 $m^2\,g^{-1}$ for sieved BR.

Under an optical microscope, the BR apatite appears to be formed of transparent platelets. Under a scanning electron microscope, BR particles appear as hexagonal-shaped and flat platelets: the mean length along the diagonals is 50 μm and the thickness about 5 μm. Observation at high resolution showed that the surface is irregular and that these particles are probably porous. MK is formed of particles of ill-defined shape, and with very disturbed and porous surfaces. The higher BET area of the BR apatite is probably explained by the porosity of its particles.

X-ray diffraction shows both apatites to be well crystallized.

2.2. Chemical analysis

The chemical composition of the starting hydroxyapatites and of the aqueous solutions during the sorption experiments was determined by inductively coupled plasma atomic emission spectrometry (ICP/AES), with a Thermo-Jarell-Ash Atomscan 25 sequential spectrometer.

2.3. X-ray diffraction

The crystal structures were determined from the diffraction line intensities collected on a step scan diffractometer fitted with a curved monochromator in the diffracted beam, a scintillation counter and a pulse-height analyser. CoK_α has been used with a scanning step of 0.05° 2θ in the range $15^\circ < 2\theta < 120^\circ$. Structure refinement was performed as already described [11] using the AFFINE [19] computer code.

2.4. Sorption experiments

The amount of cadmium retained in the solid as a function of time was determined for both apatites by batch experiments. A cadmium solution was prepared by dissolving cadmium nitrate in water. pH was adjusted to 5 by addition of nitric acid. Batches of 50 mg hydroxyapatite were introduced into 25 ml fractions of the cadmium solution. The initial cadmium to apatite ratio was 4 mol mol^{-1}. The apatite suspensions were shaken at 20 °C for times varying from 1 min to 10 d and pH measured again. After shaking, pH values were in the 5.8–6.1 range. The solutions were then filtered on a 0.2 μm porosity filter and analysed for cadmium, calcium, sodium and phosphorus by ICP/AES. The remaining concentrations of phosphorus, calcium and sodium in the solid and the concentration of sorbed cadmium, were calculated from these analyses. The solids were characterized by X-ray diffraction.

A series of experiments was also performed under the same conditions but with the cadmium solution alone in order to control possible adsorption or precipitation effects.

2.5. Nuclear microprobe analysis

Measurements were performed using the nuclear microprobe facility [20] of Pierre Sue Laboratory at Saclay, France. The proton beam was focused down to a diameter of approximately 5 μm which is small compared to the flat surface of the BR apatite particles, on which the beam was directed. Several energies were used: 0.5, 0.7, 0.9 and 2 MeV with intensities limited to 0.3 nA. Two types of spectra were collected simultaneously: X-rays were collected using a Si(Li) detector for PIXE (proton induced X-ray emission) and backscattered protons were collected using a surface barrier detector at 140° for Rutherford back-scattering spectrometry (RBS). Experimental methods and data processing have been described previously [14]. Interactive processing of PIXE and RBS data allowed us to calculate the distribution of cadmium in the solid.

2.6. Flocculation

Solutions of cadmium with a concentration of 20 mg l^{-1} ($1.8\ 10^{-4}$ mol l^{-1}) were used, together with 0.5 g l^{-1} MK apatite and 0.05 g l^{-1} alum ($Al_2(SO_4)_3$), as flocculating agent. Both demineralized and tap water were tested. The pH of the solution was modified by additions

of sodium hydroxide or nitric acid solutions, the natural pH being around 6–7. In parallel with flocculation experiments, samples for residual turbidity measurements were taken (using a ratio/XR Turbidimeter from Hach), expressed as nephelometric turbidity units (NTU).

A light scattering instrument with a flow-through detector (PDA 2000, Rank Brothers Ltd, UK) connected to a recorder, was used to monitor the dynamics of flocculation. The flocculation vessel had a content of 3 l and the apatite dispersion was driven by a peristaltic pump at a flow-rate of 34 ml min^{-1} at room temperature; after the measurement with the detector, the liquid was not recycled into the vessel. It is more convenient to divide the RMS value by the steady state direct current (d.c.) value of the transmitted light to obtain the dimentionless term $R = \text{RMS/d.c.}$, often referred to as the flocculation index. As flocculation proceeds, the value of R increases. Although, this ratio does not provide quantitative information on aggregate size, the relative increase in R value is an indicator of the degree of flocculation. For a given dispersion, it can be assumed that larger R values imply larger aggregate sizes [21, 22]. The same technique has been successfully applied to study the mechanisms of flocculation of either dilute or concentrated dispersions, adding polymeric [23] or hydrolysing metal salt flocculants [24, 25].

3. Results

3.1. Chemical composition and structure of the starting hydroxyapatites

The results obtained by ICP/AES showed (Table I) that both starting apatites are cation deficient and contain sodium, with MK apatite being close to the stoichiometric hydroxyapatite $Ca_{10}(PO_4)_6(OH)_2$. For each compound, two limiting formulae are proposed and the actual composition may be between these. This point has been discussed previously [11, 15].

The crystal structure is hexagonal ($P6_3/m$) as described in previous work [11]. The main crystallographic parameters are reported in Table I. Ca^{2+} ions occupy two different crystallographic sites. Ca(1) is found on ternary axes at $x = 1/3$, $y = 2/3$ and Ca(2) at sites with symmetry m at $z = 1/4$, $z = 3/4$. OH^- ions are found at $z = 0.198$, in channels centred on the hexagonal screw-axes. In stoichiometric apatites, 4 Ca(1) and 6 Ca(2) per unit cell are occupied. Structural refinement showed that, in BR, Ca(1) sites are almost entirely occupied, whilst Ca(2) sites are partially occupied [11]. Sites occupied by sodium could not be determined, because the concentration of this element and its electron density are too low. The number of vacancies in MK is too small to detect a partial occupancy.

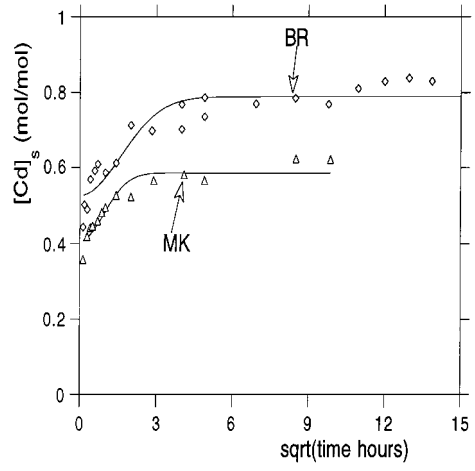

Figure 1 Sorption kinetics of cadmium on BR and MK calcium hydroxyapatities. Variation of the cadmium concentration $[Cd]_s$ in the solid (mol per mol apatite) as a function of the square root of time.

3.2. Results of batch sorption experiments

Results of sorption kinetics are reported in Fig. 1. For the same initial concentration of cadmium in solution (4 mol per mol apatite), a steady state is achieved after approximately 16 h for BR and 5 h for MK. The interpretation of this difference will be discussed later, together with the discussion of the sorption mechanisms.

Through ICP/AES analysis it was possible to establish the mass balance between the quantity of sorbed cadmium and the quantities of elements initially present in the apatite and subsequently transferred to the solution. For both apatites, the fixation of cadmium is compensated by transfer of equivalent quantities of calcium and sodium into solution, sodium being almost entirely transferred. This result is consistent with a cation exchange, but a dissolution–precipitation process may lead to the same balance.

There is a difference between the values achieved at the plateau which are about 0.8 mol mol^{-1} for BR and 0.6 mol mol^{-1} for MK. Further experiments, in which the initial concentration of cadmium in the solution varied, showed that these values are close to the maximum uptake. It has been shown that this uptake varies slightly with pH [15]. Finally, the maximum capacity that may be reached for both apatites is about 0.7–0.8 mol mol^{-1} (7×10^{-4} mol g^{-1} or 80 mg g^{-1}). This value is high enough for the use of apatites for water decontamination, but is far from the total calcium concentration or

TABLE I Chemical composition and crystallographic parameters of the starting hydroxyapatites. The composition is deduced from ICP/AES analysis, the unit cell parameters and the site occupancy from X-ray diffraction

Apatite	Limit formulae	Unit cell parameters		Site occupancy
		a (nm)	c (nm)	
BR	$Ca_{9.1}Na_{0.5}(PO_4)_6(OH)_{0.7} \cdot 4.2H_2O$ $Ca_{9.1}Na_{0.5}(PO_4)_{4.7}(HPO_4)_{1.3}(OH)_2 \cdot 2.9H_2O$	0.9436	0.6880	Ca(1) $(3.7 \pm 0.2)/4$ Ca(2) $(5.3 \pm 0.3)/6$
MK	$Ca_{9.8}Na_{0.06}(PO_4)_6(OH)_{1.6} \cdot 1.2H_2O$ $Ca_{9.8}Na_{0.06}(PO_4)_{5.6}(HPO_4)_{0.4}(OH)_2 \cdot 0.84H_2O$	0.9415	0.6879	Ca(1) $(3.9 \pm 0.2)/4$ Ca(2) $(5.8 \pm 0.3)/6$

even from the 6 Ca(2) sites per unit cell of the crystal structure. This point is discussed later.

3.3. Crystal structure after sorption

The apatitic structure is not modified and the variation of the unit cell parameters is negligible. The intensity of diffraction lines is slightly modified. Structure refinement on BR apatite has previously shown that, after sorption, cadmium is exclusively located in Ca(2) sites [11]. The same result was observed here with MK. Therefore, it seems that this site distribution is specific to sorption, because cadmium occupies both Ca(1) and Ca(2) sites in precipitated solid solutions of Cd–Ca apatites [26, 27].

3.4. Distribution of sorbed cadmium in the solid

Scanning electron microscope imaging showed that the morphology of the BR apatite is not modified by the sorption of cadmium. No other solid which could result from a precipitation was detected.

There is no significant variation of the position and width of the X-ray diffraction lines. The variations of cell parameters in Cd–Ca hydroxyapatites prepared by precipitation, which show solid solution in the full range of concentrations, are known [26]. Between 0 and 0.8 mol mol^{-1}, the variation is not expected to be significant. Our results indicate that the distribution is relatively uniform and exclude the existence of zones of highly cadmium-enriched apatites, otherwise there would have been a significant variation of cell parameters, resulting in the displacement or deformation of the diffraction lines.

Several samples of the starting BR apatite and of the apatite containing cadmium were irradiated in the nuclear microprobe by a proton beam perpendicular to the flat surface of the platelets. PIXE showed that the mean concentration of cadmium is in agreement with the ICP/AES analysis. The absence of a characteristic peak in the RBS spectrum, clearly showed that there is no accumulation of cadmium on the surface. On the contrary, cadmium is distributed throughout the whole thickness of the particles. Results of modelling the RBS spectra using distribution functions showed the gradient to be small. Generally, the concentration is lower in the middle of the samples than in the superficial part by a factor of 2. An example is given in Fig. 2. We attempted to model the concentration gradient by a diffusion process and diffusion coefficients were calculated. Depending on the contact time between the apatite and the solution, values ranging from 10^{-10}–10^{-12} cm^2 s^{-1} were obtained. These values indicate a rather rapid diffusion at room temperature. Literature values of diffusion coefficients in apatites are available for strontium and lead [28–31]. Diffusion coefficients smaller than 10^{-14} cm^2 s^{-1} are reported for temperatures as high as 900 °C, but these results are not quite comparable to ours, because they were obtained for fluorapatites rather than hydroxyapatites. The diffusion conditions were also different: hydrothermal [29],

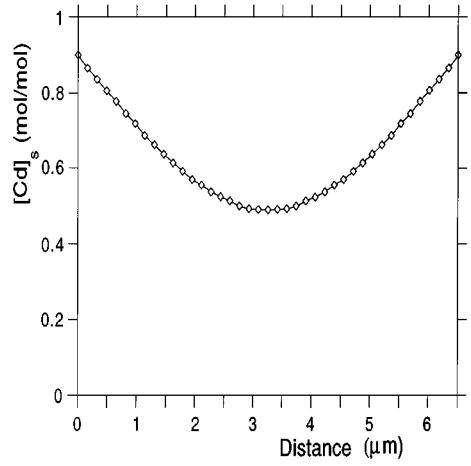

Figure 2 Example of the distribution of cadmium along the *c*-axis in a crystal of BR hydroxyapatite, calculated by fitting the spectrum of backscattered protons. The concentration $[Cd]_s$ is expressed in mol per mol apatite as a function of the distance from the surface for a crystal 6.5 μm thick.

in molten salts [28] or by implantation [30, 31], while we have worked with aqueous solutions with relatively high concentrations of cadmium. Strontium and lead have larger ionic radii than calcium, whilst that of cadmium smaller. In our case, diffusion could be enhanced by the porosity detected by the BET measurements. However, the large variations of the diffusion coefficient that we observed indicate that this is not a simple diffusion process. The smallest measured values correspond to the longest contact times. This variation may be related to a coefficient decreasing with increasing cadmium concentrations, or complex diffusion mechanisms including a surface barrier. The present results are not sufficient to allow us to come to any conclusion.

Microprobe measurements have not been applied to MK, as the particle diameters of this apatite were too small. However, similar sorption capacity values and crystal structure results indicate that cadmium probably also penetrates the solid.

3.5. Separation of phases by flocculation

During preliminary experiments in deionized water, the effect of flow rate of the dispersion of MK hydroxyapatite without cadmium through the cell was evaluated (Table II). The maximum flocculation index, implying larger aggregates, was obtained after 8 min at natural pH (5.5–6.5), employing a flow rate of 46 l min^{-1}. In sheared dispersions it is likely that a given particle

TABLE II Flocculation of hydroxyapatite particles by aluminium sulphate without cadmium (duration of rapid mixing 120 s, natural pH 5.5–6.5). Influence of different flow rates of the dispersion through the flow cell on the maximum obtained values for *R* ratios and the respective agitation times

Flow rate of the dispersion (ml min^{-1})	Max. value of *R* ratios
22	1.05 (5 min)
33.5	1.44 (9 min)
46	1.89 (8 min)
58	1.48 (7 min)
69	1.32 (4 min)

TABLE III Flocculation of hydroxyapatite particles by aluminium sulphate without cadmium or recycling (flowrate 34 ml min^{-1}, natural pH 5.5–6.5). Influence of mixing intensity during flocculation on *R* ratios, applying preliminary rapid mixing for 30 s

Mixing intensity (r.p.m.)	Max. value of *R* ratios
62	1.84 (6 min)
100	2.68 (5 min)
200	2.84 (5 min)
300	2.55 (4 min)
400	2.13 (3 min)
600	1.44 (2 min)

would undergo several collisions with other particles, before it had acquired enough flocculant ions to allow aggregates to form. This effect can be seen experimentally as a "lag phase" between the addition of flocculant agent and the onset of flocculation. It can be noticed also that under conditions of high shear and especially in turbulent flow, there is a possibility of floc breakage–destruction as a result of shear forces at the particle surface. In certain experiments the flocculation indices did not change significantly with time, indicating that the rates of aggregation and floc breakage were comparable.

The influence of the intensity of mixing (expressed in terms of r.p.m. of the mechanical mixer) on hydroxyapatite flocculation by alum is shown in Table III. At this range of mixing intensity, the flocculation rate increased with the number of r.p.m., because of the increase in the collision rate of the flocculant precipitates and the particles up to 200 r.p.m.

At lower mixing velocities (up to 100 r.p.m.), the decrease in the value of the flocculation index was devoted to the settling of large aggregates/flocs during the flocculation process, as it was difficult to keep the large flocs dispersed in the water. Therefore, the number of particles sampled by the inserted plastic tube, leading to the photo dispersion analyser, was found to be decreased. Because the flocculation index is proportional to the particle size and to the square root of particle concentration [21], the flocculation index decreased as fewer particles enter the sampling tube. At higher mixing velocities (300–600 r.p.m.), the flocculation indices attained limiting values at an earlier stage (2–4 min) instead of 5 min, i.e. the more rapid the stirring, the shorter the "lag phase." When the mixing intensity was also increased, the initial slope of the flocculation index curves was noticed to be increased, indicating higher aggregation rates; this was caused by increased particle collision rate. In addition, the maximum *R* values increased up to a certain mixing intensity and then were observed to be decreased. The flocs reached a limiting size and although they were not noticed to be settled at higher mixing intensities, their breakage by fluid shear forces was more dominant over the aggregates growth (after the initial flocculation period), hence their size and the respective *R* values were decreased.

Experiments were performed to study the influence of pH and time on the flocculation of MK apatite without cadmium (Figs 3 and 4). The influence of Cd and

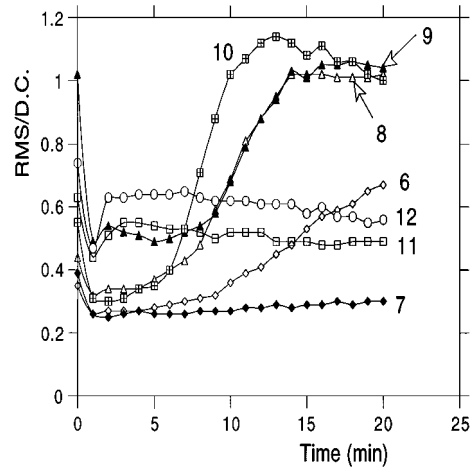

Figure 3 Influence of contact time on the flocculation of MK hydroxyapatite for various pH values. The flocculation index is expressed as the RMS/d.c. ratio. pH: (◆) 7, (△) 8, (▲) 9, (⊞) 10, (□) 11, (◯) 12.

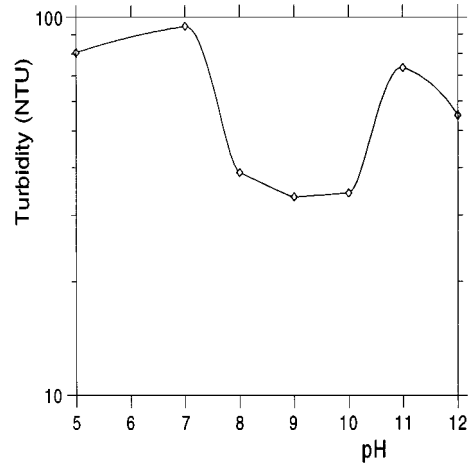

Figure 4 Influence of pH on the turbidity during flocculation experiments with MK hydroxyapatite.

water quality is presented in Fig. 5, while the influence of flocculant concentration is shown in Fig. 6. The RMS/d.c. ratio reached maximum values, i.e. good flocculation occurs, after reasonably short times for a pH range of 8–10. Meanwhile, the turbidity was reduced

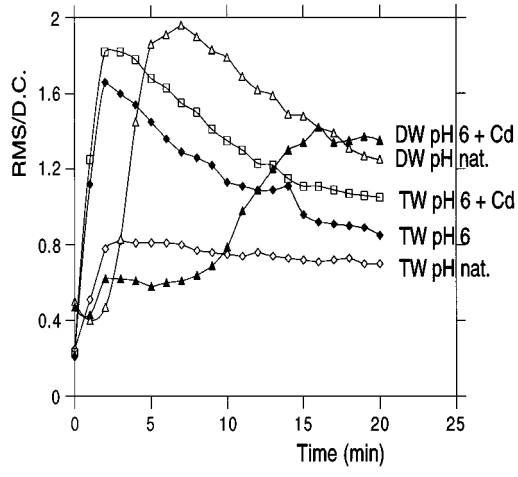

Figure 5 Influence of contact time on the flocculation of MK hydroxyapatite with the effect of water quality, pH and the presence or absence of cadmium (DW, demineralized water; TW, tap water; pH nat., natural pH). The flocculation index is expressed as the RMS/d.c. ratio.

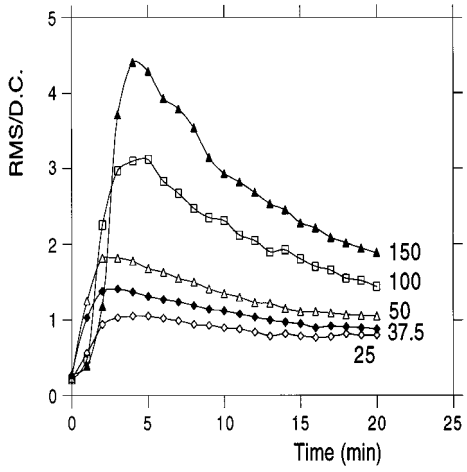

Figure 6 Influence of contact time and concentration of flocculant on the flocculation of MK hydroxyapatite. The flocculation index is expressed as the RMS/d.c. ratio. Flocculant concentration (alum): (◇) 25 mg l^{-1}, (◆) 375 mg l^{-1}, (△) 50 mg l^{-1}, (□) 100 mg l^{-1}, (▲) 150 mg l^{-1}.

in this pH range under 40 NTU. By increasing the flocculant concentration up to 150 mg l^{-1}, the ratio was found to increase further. With this concentration, the use of tap water instead of demineralized water did not significantly affect the results.

The inorganic flocculant used in these experiments hydrolyses in solutions near neutral pH, and the hydrolysis products, which have a positive surface charge, are strongly sorbed by solids. From our experience with other minerals [32], the effects of solubility of these materials need special attention and the solution conditions usually explain their behaviour (sorption, precipitation, etc.).

These results showed that the flocculation process can be successively applied to hydroxypatites because RMS/d.c. values greater than 3 can be achieved. This result, combined with the high removal efficiency of these sorbents for cadmium, is promising for the separation of cadmium-loaded small-size particles of apatite.

4. Discussion

The main results concerning the sorption mechanisms, are that (i) cadmium ions penetrate into the bulk of the solid, and (ii) the shape of the solid and its structure are not modified, except that some Ca(2) sites are substituted by cadmium. These results suggest that the main sorption mechanism is diffusion and ion exchange, excluding precipitation. Ion exchange leads to the formation of a (Cd–Ca) solid solution. Different results were obtained in the case of the sorption of lead and uranium on the same BR apatite [33]. For these two elements, sorption leads to precipitation of other solid phases. This difference in behaviour is probably related to the ionic radii of the ions: cadmium ions have a radius close to calcium but slightly smaller, whilst lead and uranyl ions have larger radii [34], thus permitting easier diffusion of cadmium into the solid. Such a diffusion mechanism may explain the difference in sorption kinetics between the BR and MK apatites, as already mentioned: the smaller particles of MK apatite need less time to reach a steady state of diffusion than the larger particles of BR.

However, some points remain unexplained. One of these is the limitation of the sorption capacity to 0.8 mol mol^{-1}, which is a small part of the 6 "available" Ca(2) sites of the unit cell. One reason may be an intrinsic property of cadmium not to occupy a site close to another already occupied by the same cation. This hypothesis may be compared to the results obtained on the superficial sorption of cadmium on ferric oxides: cadmium ions never associate to give multinuclear surface species [35]. Such limitation may also explain the variation of calculated diffusion coefficients. The most probable pathways for diffusion are the channels centred on the hexagonal screw-axes. As already noticed, exchange of cadmium occurs only with Ca(2) sites adjacent to these channels, while Ca(1) sites are less accessible. In the course of the exchange, as more and more sites are occupied by cadmium, the tendency not to occupy adjacent sites would lower the possibility of exchange and, therefore, the diffusion coefficient will decrease. This hypothesis has to be verified by complementary experiments.

Thus, sorption of cadmium proceeds by an exchange process. However, this result does not mean that this process can be modelled by an ion-exchange equilibrium. As is suggested by the limited number of exchange sites compared to the available ones and by the concentration gradient observed by the nuclear microprobe, a true exchange equilibrium is certainly not achieved. This gradient is still observed after the longest contact times, resulting in the already mentioned decrease of calculated diffusion coefficients with time. Therefore, the steady state value observed in the sorbed concentration of cadmium is probably controlled not by ion exchange but by diffusion. Complementary experiments on the reversibility of sorption confirmed that sorption does not proceed as a reversible equilibrium. Results showed that, after 48 d contact with a solution containing 4 mol Ca per mol apatite, only 15% of the cadmium initially present in the solid is released into the solution.

As shown in our earlier work [15], the number of cationic sites depends on the pH, due to a protonation–deprotonation equilibrium

$$HPO_4^{2-}\ (\text{apatite}) \rightleftharpoons H^+\ (\text{solution}) + PO_4^{3-}\ (\text{apatite}) \quad (1)$$

The presence of cadmium tends to shift this equilibrium to the right side [15]. This process has to be considered in addition to the pure Ca–Cd exchange.

5. Conclusion

This work contributed both to a better understanding of the mechanisms of cadmium sorption on hydroxyapatites and to the use of such material for the decontamination of waters and industrial effluents. Concerning this last point, a removal efficiency higher than 99.5% was observed. A subsequent separation of the cadmium-loaded solid by flocculation is a promising method. The fact that cadmium is incorporated into the bulk of the apatite with partial reversibility is important

in the context of the safe storage of used sorbent material. Further experiments are planned to elucidate the diffusion mechanism and the causes of the limitation of the sorption capacity. Further developments are also needed in the use of apatites for treatment of contaminated waters or as artificial barriers disposed around contaminated areas.

Acknowledgements

This work has been supported by European Union "Human Capital and Mobility Programme" entitled "Mechanisms of Sorption of Priority Pollutants from Aqueous Solutions onto New Inorganic Sorbents" (Contract no. ERB CHRXTCT 930272). It was also performed in the framework of the PRACTIS programme (Physico-Chimie des Actinides et autres Radioéléments dans les Solutions et aux Interfaces).

References

1. G. N. BATURIN and V. N. ORESHKIN, *Geochem. Int.* **35** (1984) 69.
2. T. MIYAHARA, M. MIYAKOSHI, Y. SAITO and H. KOZUKA, *Toxicol. Appl. Pharmacol.* **55** (1980) 477.
3. J. CHRISTOFFERSEN, M. R. CHRISTOFFERSEN, R. LARSEN, E. ROSTRUP, P. TINGSGAARD, O. ANDERSEN and P. GRANDJEAN, *Calcif. Tiss. Int.* **42** (1988) 331.
4. J. SANTILLAN-MEDRANO and J. JURINAK, *Soil Sci. Soc. Am. Proc.* **39** (1975) 851.
5. N. NAYAK and B. V. C. RAO, *J. Indian Chem. Soc.* **53** (1976) 630.
6. T. SUZUKI, T. HATSUSHIKA and Y. HAYAKAWA, *J. Chem. Soc. Farad. Trans. I* **77** (1981) 1059.
7. Y. TAKEUCHI and H. ARAI, *J. Chem. Eng. Jpn.* **23** (1990) 75.
8. T. SUZUKI, T. HATSUSHIKA and M. MIYAKE, *in* "Proceedings of the International Conference on New Developments in Ion Exchange," Tokyo, Japan, 2–4 October 1991, p. 401.
9. J. J. MIDDELBURG and R. N. J. COMANS, *Chem. Geol.* **90** (1991) 45.
10. Q. Y. MA, S. J. TRAINA, T. J. LOGAN and J. A. RYAN, *Environ. Sci. Technol.* **27** (1993) 1803.
11. U. VINCENT, J. JEANJEAN and M. FEDOROFF, *J. Solid State Chem.* **108** (1994) 68.
12. Y. XU, F. W. SCHWARTZ and S. J. TRAINA, *Environ. Sci. Technol.* **28** (1994) 1472.
13. S. MANDJINY, A. I. ZOUBOULIS and K. A. MATIS, *Separ. Sci. Technol.* **30** (1995) 2963.
14. N. TOULHOAT, V. POTOCEK, C. NESKOVIC, M. FEDOROFF, J. JEANJEAN and U. VINCENT, *Radiochim. Acta.* **74** (1996) 257.
15. J. JEANJEAN, M. FEDOROFF, F. FAVERJON, U. VINCENT and J. CORSET, *J. Mater. Sci.* **31** (1996) 6156.
16. S. K. DENTEL, *Crit. Rev. Envir. Control* **21**(1) (1991) 41.
17. K. KOBAYASHI, *Bull. Chem. Soc. Jpn.* **48** (1975) 1750.
18. A. I. ZOUBOULIS and K. A. MATIS, *Water Sci. Tech.* **31** (3–4) (1995) 315.
19. W. R. BUSING, K. O. MARTIN and H. A. LEVY, "A Crystallographic Least Square Program ORFLS AFFINE" (1984).
20. C. ENGELMANN and G. REVEL, *Nucl. Instrum. Meth. B* **54** (1991) 84.
21. J. GREGORY, *J. Coll. Interface Sci.* **105** (1985) 357.
22. J. GREGORY and D. W. NELSON, *Coll. Surfaces* **128** (1986) 175.
23. J. GREGORY and S. Y. LEE, *J. Water SRT-Aqua* **39** (1990) 265.
24. H. W. CHING, T. S. TANAKA and M. ELIMELECH, *Water Res.* **28** (1994) 559.
25. H. W. CHING, M. ELIMELECH and J. G. HERING, *ASCE J. Envir. Eng.* **120** (1994) 169.
26. A. NOUNAH, J. SZILAGYL and J. L. LACOUT, *Ann. Chim. Fr.* **15** (1990) 409.
27. A. NOUNAH, J. L. LACOUT and J. M. SAVARIAULT, *J. Alloys Compounds* **188** (1992) 141.
28. E. B. WATSON, T. M. HARRISON and F. J. RYERSON, *Geochem. Cosmochim. Acta* **49** (1985) 1813.
29. J. R. FARVER and B. J. GILETTI, *ibid.* **53** (1989) 1621.
30. D. J. CHERNIAK, W. A. LANFORD and F. J. RYERSON, *ibid.* **55** (1991) 1663.
31. D. J. CHERNIAK and F. J. RYERSON, *ibid.* **57** (1993) 4653.
32. K. A. MATIS and G. P. GALLIOS, *Int. J. Min. Process* **25** (1989) 261.
33. J. JEANJEAN, J. C. ROUCHAUD, L. TRAN and M. FEDOROFF, *J. Radioanal. Nuclear Chem. Lett.* **201** (1995) 529.
34. R. D. SHANNON, *Acta Crystallogr. A* **32** (1976) 751.
35. L. SPADINI, A. MANCEAU, P. W. SCHINDLER and L. CHARLET, *J. Coll. Interface Sci.* **168** (1994) 73.

Received and accepted 23 July 1998